Journal of PHYCOLOGY

An International Journal of Algal Research

VOLUME 43
NUMBER 2
APRIL 2007

A Publication of the Phycological Society of America

J. Phycol. **43,** 319–332 (2007)

DOI: 10.1111/j.1529-8817.2007.00324.x

LIGHT AND ELECTRON MICROSCOPE OBSERVATIONS OF *ALGIROSPHAERA ROBUSTA* (PRYMNESIOPHYCEAE)[1]

Ian Probert[2]

Station Biologique de Roscoff, Place Georges Teissier, 29682 Roscoff, France
Algobank Microalgal Culture Collection, University of Caen, 14032 Caen, France

Jacqueline Fresnel, Chantal Billard

Laboratoire de Biologie et Biotechnologies Marines, Université de Caen, 14032 Caen, France

Markus Geisen

Alfred Wegener Institute, Am Handelshafen 12, D-27570 Bremerhaven, Germany

and

Jeremy R. Young

Palaeontology Department, The Natural History Museum, Cromwell Road, London SW7 5BD, UK

The coccolithophore *Algirosphaera robusta* (Lohmann) R. E. Norris was isolated into laboratory culture for the first time. This species is of particular interest as the first deep photic coccolithophore to be cultured, the only member of the Rhabdosphaeraceae to have been successfully isolated, and the first coccolithophore with a coccolith structure including a complex disjunct central area to have been studied in detail. Observations on the culture strain supported the previous inference that the commonly recognized species *A. robusta*, *A. oryza* Schlauder, and *A. quadricornu* (J. Schiller) R. E. Norris are conspecific. However, *A. meteora* (Müller) R. E. Norris and *A. cucullata* (Lecal-Schlauder) J. R. Young, Probert et Kleijne were recognized as discrete species. Coccolith rim formation in *A. robusta* follows the pattern of biomineralization documented in other heterococcoliths and was suggested to be universal. However, the prominent central hood had a unique ultrastructure and appeared to be formed by a distinctively different biomineralization mode. We suggest that this can provide a key to reinterpreting homology in coccolith structure and that this species is a promising target for comparative biochemical and genomic studies of biomineralization. In terms of cell ultrastructure, *A. robusta* exhibited marked similarities to *Syracosphaera pulchra* Lohmann, and a close evolutionary relationship between the families Rhabdosphaeraceae and Syracosphaeraceae is suggested.

Key index words: **biomineralization; coccolithophore; Haptophyta; Prymnesiophyceae; taxonomy; ultrastructure**

Coccolithophores are the most prominent members of the haptophyte algae, an important group of primary producers and key sediment formers. As a result, they have attracted considerable interdisciplinary interest over the past decade, with extensive study of their biogeography, biochemistry, and biogeochemical role. This recent interest has not, however, been matched by a comparable range of classical phycological, and in particular cytological, studies. Some 200 species of coccolithophores have been described in 13 families (Jordan and Green 1994, Young et al. 2003), but relatively few detailed cytological studies have been published, due primarily to the limited availability of members of this group in culture. These studies have nevertheless yielded invaluable phylogenetic information and indicated significant diversity, notably in modifications of the Golgi system related to coccolith biomineralization and in the structure of the flagellar/haptonematal basal complex. Consequently, there is considerable potential for further studies to probe the high-level cytological diversity within the coccolithophores.

The coccolithophore *Algirosphaera robusta* was recently isolated into clonal laboratory culture. This is, to our knowledge, the first successful culture not only of this species, but of any member of the family Rhabdosphaeraceae Haeckel. *Algirosphaera robusta* is a common coccolithophore with a wide biogeographical range, having been recorded in the North Atlantic, Mediterranean Sea, Red Sea, Indian Ocean, and central Pacific (Kleijne 1992). The highest abundances

[1]Received 20 June 2006. Accepted 21 December 2006.
[2]Author for correspondence: e-mail probert@sb-roscoff.fr.

of this species are typically observed in the lower photic zone (Okada and McIntyre 1977). The Rhabdosphaeraceae includes only 15 described extant species, but these show spectacularly diverse morphology and are assigned to seven genera. The taxonomy of this family has been reviewed by Norris (1984), Kleijne (1992), and most recently by Aubry (1999). Strong similarities are evident in the basic structure of coccoliths (particularly of the coccolith rim) between the various species, and the grouping is not in dispute. The coccoliths are typically disk-shaped (planoliths) and formed of three components: (1) a narrow, slightly elevated rim formed of an upper rim cycle of simple nonimbricate elements and a lower rim cycle showing strong obliquity; (2) a radial cycle of laths (of equal number to the rim units) typically with slits between the laths; (3) the radial cycle joins the rim to a central lamellar cycle consisting of numerous small elements with a more or less clear helical arrangement, which forms diverse central structures and may end in a cuneate cycle of a few well-formed elements (Kleijne 1992). The extant Rhabosphaeraceae mostly form very small coccoliths (typically the bases have a diameter of <3 μm) and have a very limited fossil record, except for *Rhabdosphaera clavigera* [var. *clavigera* Murray et Blackman, var. *stylifera* (Lohmann) Kleijne et R. W. Jordan], which is present through the Neogene to about 24 Ma (Young 1998). In the Eocene (55–38 Ma), however, a diverse group of larger species occurred (Perch-Nielsen 1985, Shafik 1989, Varol 1989, Aubry 1999). These species had similar rims and radial cycles to the extant species, but highly variable, often multitiered, central structures.

Young et al. (1992) proposed a general model for heterococcolith biomineralization with a conserved pattern of growth from a protococcolith ring of calcite nuclei with alternating vertical and radial *c*-axes. This "V/R model" has been well supported by subsequent studies (Young 1993, Marsh 1999, Young et al. 1999, 2004). The rim structure of heterococcoliths of the Rhabdosphaeraceae appears to fit this model, but the development of the central area lamellar and cuneate cycle elements remains obscure (Kleijne 1992). Hence, a key objective of this study was to determine the relationship between the biomineralization of the central process and that of the coccolith rim. The Syracosphaeraceae (Lohmann) Lemmerm. and Calciosoleniaceae Kamptner appear to have a radial cycle similar to that of the Rhabdosphaeraceae, which suggests affinities between these three families (Young 1998, Young et al. 2004). Detailed analysis of the structure of *Syracosphaera pulchra* by Inouye and Pienaar (1988) and Young et al. (2004) has shown that this radial cycle originates in the protococcolith ring that forms the rim, but via separate nucleation, with tangential *c*-axis orientation. Possession of this cycle appears to be an important homology separating these three families from other heterococcoliths, which have distinctly simpler structures. In consequence, the three families were placed in the order Syracosphaerales in the revised classification of Young et al. (2003).

The type species of *Algirosphaera*, the heterococcolith-bearing *A. oryza* (designated by Loeblich and Tappan 1963), was transferred to *Anthosphaera* Kamptner by Gaarder and Hasle (1971), and *Algirosphaera* became a junior synonym of *Anthosphaera*. When the type species of *Anthosphaera* proved to have holococcoliths, Norris (1984) transferred all heterococcolith-bearing *Anthosphaera* species to *Algirosphaera* and gave an emended description of this genus (see Aubry 1999 for an exhaustive discussion of the taxonomy of these genera). Halldal and Markali (1955) considered *Algirosphaera* coccoliths to be rhabdoliths, and the genus has been placed in the Rhabdosphaeraceae in most of the recent literature, although Tappan (1980) and Steinmetz (1991) included it in the Syracosphaeraceae, following Kamptner (1941). Eight species of *Algirosphaera* have been described (Kleijne 1992, Aubry 1999), the majority of which are now considered to be synonyms. Halldal and Markali (1955) distinguished three species based on coccosphere shape and coccolith arrangement. This system has been widely followed and is summarized by Heimdal (1993): *A. oryza* is described as having flattened ellipsoidal coccospheres with two rows of equatorial coccoliths projecting approximately at right angles to each other giving the coccosphere a "coronate" profile. *Algirosphaera quadricornu* has ellipsoidal coccospheres, and *A. robusta* spherical coccospheres. Ordinary (i.e., body as opposed to stomatal) coccoliths of *A. oryza* and *A. quadricornu* are indistinguishable (1.8–2.4 μm high), while those of *A. robusta* are markedly lower (1.5 μm high). In distal view, the outline of the coccoliths in *A. oryza* and *A. quadricornu* are elliptical compared with the nearly parallel long sides in *A. robusta*. Kleijne (1992) merged all *Algirosphaera* species into *A. robusta* on the grounds that body rhabdoliths showing the characteristics of *A. robusta, A. oryza*, and *A. quadricornu* are often observed to occur together on the same coccosphere. She noted, however, that given the wide biogeographic range of these species and the morphological variability observed, it was possible that detailed examination might lead to the recognition of discrete species. In the recent literature, some authors have continued to use the species *A. oryza* or *A. quadricornu* (Hagino et al. 2000, Jordan and Winter 2000).

In this paper, we present LM observations of cell morphology and behavior, SEM observations of coccolith morphology and ultrastructure, and a TEM study of the fine structure of the cell and coccolith formation. In addition, this culture strain has been included in several multispecies studies of diverse aspects of coccolithophore biology, including molecular phylogeny (Sáez et al. 2004), pigment composition (van Lenning et al. 2004), strontium incorporation into coccolith calcite (Stoll et al. 2002), and stable isotope fractionation in coccoliths (Ziveri et al. 2003).

MATERIALS AND METHODS

The culture (strain AC503, Algobank-Caen culture collection, University of Caen, France) was initiated from a single cell isolated from a concentrated water sample collected at station 64 (37°24.38′ N, 0°56.1′ W) during the MATER II cruise in the Alboran Sea in October 1999. The water was collected in Niskin bottles from the subsurface chl maximum at 37 m depth. The culture was routinely maintained at 17°C in a filter-sterilized K/2 (-Si,-Tris) medium (Keller et al. 1987) with daylight fluorescent tubes providing an irradiance of 50 μmol photons $\cdot m^{-2} \cdot s^{-1}$ with a photoperiod of 16:8 light: dark (L:D).

The LM observations on living cells were conducted with a Leitz Orthoplan microscope (Leitz, Wetzlar, Germany) equipped with differential interference contrast (DIC) optics. A Zeiss Axioplan microscope (Zeiss, Jena, Germany) was used for cross-polarized light observations on coccoliths. To obtain information on coccolith ultrastructure, both culture samples and wild samples from the western Mediterranean were examined. Culture material was observed in the medium, whereas for filtered wild samples, a piece of the 0.45 μm pore-size cellulose nitrate filter (Whatman, Brentford, UK) was mounted with immersion oil on a microscope slide. For SEM, drops of cell suspension concentrated on Isopore filters (Millipore, Billerica, MA, USA) were mounted on specimen stubs, coated in a Cressington 208HR sputter coater (Elektronen Optik Service GmbH, Dortmund, Germany) with 20 nm of gold/palladium (95:5%), and viewed with a Philips XL30 field emission scanning electron microscope (Philips Electronics B.V., Eindhoven, the Netherlands). For shadowed/negative-stained preparations, drops of cell suspension fixed with 2% osmium tetroxide were placed on formvar-coated grids and, after drying, rinsed with neutralized distilled water. The grids were then either shadowed with gold/palladium or stained with 2% uranyl acetate for 5 min and rinsed in distilled water. In preparation for sectioning, a cell suspension was gently centrifuged, and the pellet fixed for 1.5 h at 4°C in a glutaraldehyde solution (2.5%) in 0.1 M sodium cacodylate buffer (pH 7.2) containing 0.25 M sucrose (the fixative was prepared just before usage). Cells were then washed three times in 0.1 M cacodylate buffer containing decreasing concentrations of sucrose (0.25, 0.12 M, the last wash with no sucrose) for 15 min each time, followed by postfixation in 2% osmium tetroxide in 0.1 M cacodylate buffer for 1 h at 4°C. After washing in distilled water, cells were embedded in 2.5% agar, dehydrated in a graded ethanol series, and embedded in Spurr's resin. Sections were double stained with 2% uranyl acetate followed by Reynold's lead citrate. To preserve the mineral component of coccoliths, some sections were gathered on a solution containing 0.1 M sodium cacodylate and 0.01 M calcium chloride at pH 7.8 and observed without having been contrasted (Outka and Williams 1971). Polysaccharide localization in ultrathin sections was based on the PA–TCH–SP (periodic acid–thiocarbohydrazide–silver proteinate) staining method of Thiery (1967). Sections mounted on formvar coated gold grids were treated consecutively with the following reagents: 1% PA in aqueous solution (25 min); several rinses in distilled water; 1% TCH in 20% acetic acid (24–72 h); rinses in 10, 5, and 2% acetic acid followed by distilled water; 1% SP in aqueous solution (30 min); several rinses in distilled water. As a control, the PA step was omitted. Shadowed/negative-stained preparations and thin sections were viewed with a JEOL 100C TEM (JEOL, Tokyo, Japan).

RESULTS

Light microscopy: In culture, the coccosphere of *A. robusta* is typically flattened ellipsoidal in shape (Fig. 1a), measuring ~9 × 6 × 4 μm, but more or less spherical coccospheres (Fig. 1b), and transitions between these shapes are also observed. In old cultures, irregularly shaped coccospheres are also frequently observed. The dimorphic coccosphere consists of 30–55 irregularly positioned dome-shaped coccoliths, with larger petalloid stomatal coccoliths around the flagellar opening (Fig. 1c). The protoplast completely fills the coccosphere with a single bilobed chloroplast located in the anterior part of the cell (Fig. 1, a and b). Each cell possesses two flagella of nearly equal length, measuring 11–16 μm, and a prominent haptonema, 4–7 μm in length, with a slightly bulbous tip (Fig. 1, b and d). During rapid swimming, the flagellar opening is positioned anteriorly, the flagella trailing along the sides of the cell and the haptonema maintained straight forward (Fig. 1d), the cell swimming with a clockwise corkscrew motion in the direction of movement. When cells swim more slowly, the flagella and haptonema are often directed backward. *Algirosphaera robusta* exhibits a weakly positive phototactic response (i.e., cells tend to accumulate on the illuminated side of culture flasks), but this tendency is less pronounced than in most motile coccolithophores we have observed in culture. Cell division is initiated when the flagella and haptonema replicate and the single chloroplast divides. The pairs of flagella remain relatively close as cytokinesis splits the cell vertically, producing daughter cells of roughly equal size (Fig. 1e). *Algirosphaera robusta* is capable of rapid population growth in culture (up to 1 division $\cdot d^{-1}$ under certain conditions) and exhibits a wide temperature tolerance, growing well at both 10°C and 27°C (the extremes tested). Sexual reproduction has thus far not been observed in this culture strain.

Electron microscopy. Periplast structure: The cell covering consists of the cell membrane, an uneven layer of columnar material, several layers of small body scales, and a single layer of large coccoliths (Fig. 1f). The body scales, which consistently occur in several layers in the spaces between the coccoliths (but rarely directly underneath them), and which are particularly abundant in the region of the flagellar insertion, are elliptical (0.16–0.20 μm long × 0.09–0.11 μm wide), with an elevated rim and accentuated central ridges dividing the scale into quarters (Fig. 1, g–j). Owing to the extremely small size of these scales, it is difficult to clearly observe the fine pattern on the surface of the body scales, but negatively stained preparations and glancing sections reveal the presence of fine-radiating microfibrils in each quadrant (Fig. 1, g–i). The scales show a strong positive reaction to Thiery staining, indicating their polysaccharidic nature (Fig. 1j). The columnar material present between the coccoliths/body scales and the cell membrane is similar in structure to that seen in other coccolithophores. Coccolith base-plate scales are well developed and are visible in TEM sections and even in high-resolution SEM micrographs of the proximal surface of isolated coccoliths, although

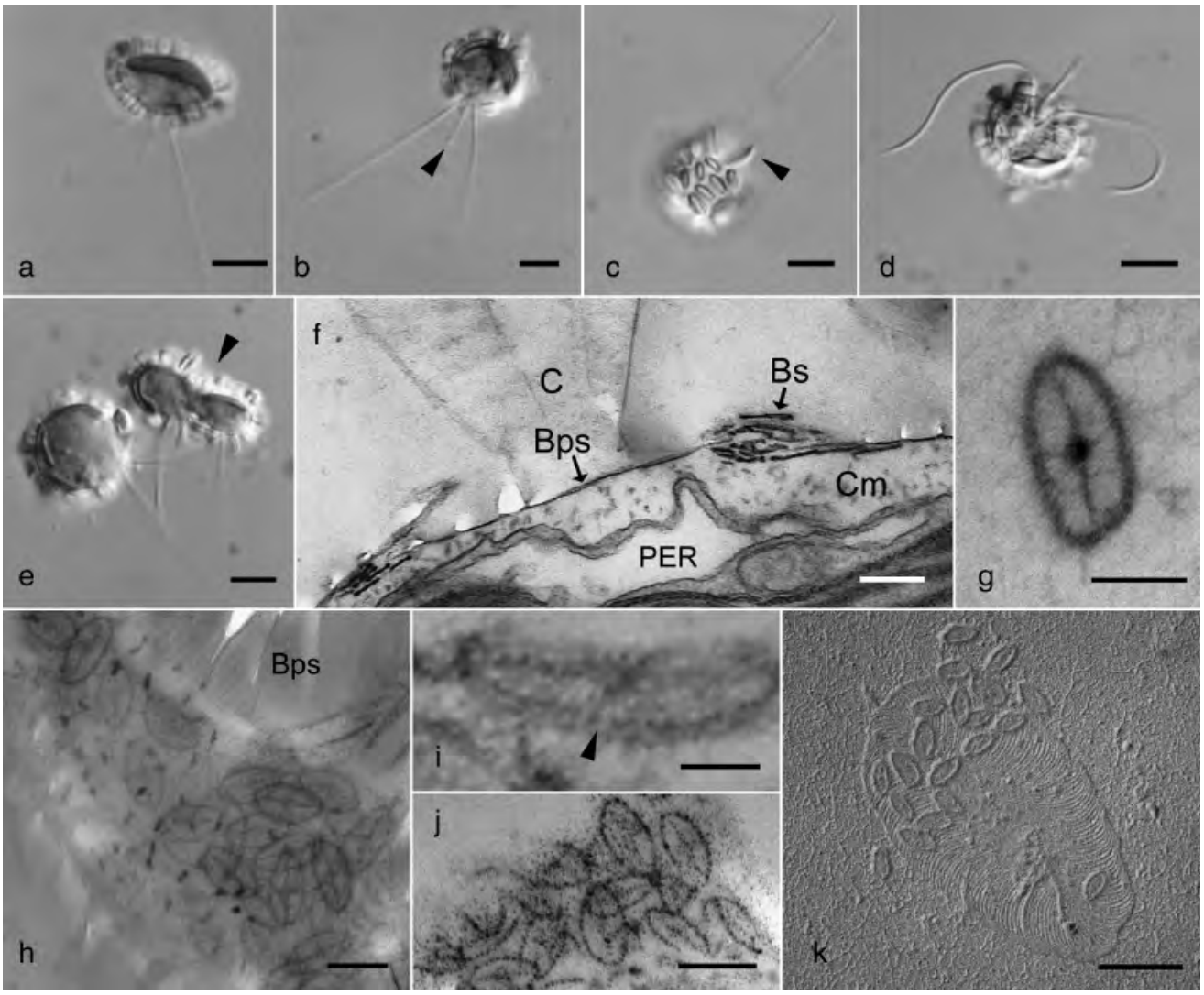

FIG. 1. *Algirosphaera robusta*. LM (differential interference contrast): (a–e); TEM: (f–k). (a) Flattened ellipsoidal cell. Scale bar, 5 μm. (b) Spherical cell with two flagella and a prominent haptonema (arrowhead). Scale bar, 5 μm. (c) Surface view of coccosphere showing body coccoliths and larger stomatal coccoliths (arrowhead) around flagellar opening. Scale bar, 5 μm. (d) Typical disposition of flagellar apparatus during swimming. Scale bar, 5 μm. (e) Dividing cell (arrowhead). Scale bar, 5 μm. (f) Thin section of periplast showing a coccolith (C) with a base-plate scale (Bps), layers of body scales (Bs), columnar material (Cm), and peripheral endoplasmic reticulum (PER). Scale bar, 0.5 μm. (g) Negatively stained preparation of a body scale. Scale bar, 0.1 μm. (h) Glancing section of a coccolith base-plate scale (Bps) and numerous small body scales. Scale bar, 0.2 μm. (i) Detail of a glancing section of a body scale with elevated rim (arrowhead). Scale bar, 0.05 μm. (j) Periodic acid–thiocarbohydrazide–silver proteinate-stained body scales. Scale bar, 0.2 μm. (k) Shadowcast decalcified preparation showing a single coccolith base-plate scale in proximal view with radial fibrils, and several smaller body scales. Scale bar, 0.5 μm.

clearest observations were possible on shadow-coated preparations of isolated scales after calcite dissolution (Fig. 1k). They are broadly elliptical in shape, measuring 2–3 μm × 1–2 μm. A pattern of radiating microfibrils divided into quadrants is observed on the proximal face, while the distal face is amorphous in structure. These scales extend to the outer margin of the coccolith, rather than being confined to the central area.

The monothecate coccosphere consists of two types of coccoliths (rhabdoliths), those covering most of the cell surface being sacculiform, with usually three higher petalloid stomatal coccoliths located around the flagellar insertion (Fig. 2a), these being curved such that they can neatly interconnect. Sometimes two or three other less-elevated coccoliths with similar appearance to the main stomatal coccoliths occur near the flagellar area, possibly representing previous stomatal coccoliths that have been subsequently replaced by larger ones. In certain specimens the coccosphere partially collapsed during preparation for SEM, which sometimes led to the observation of a coronate profile (Fig. 2b). In distal view, the outline of individual body coccoliths of this culture strain varies from more or less

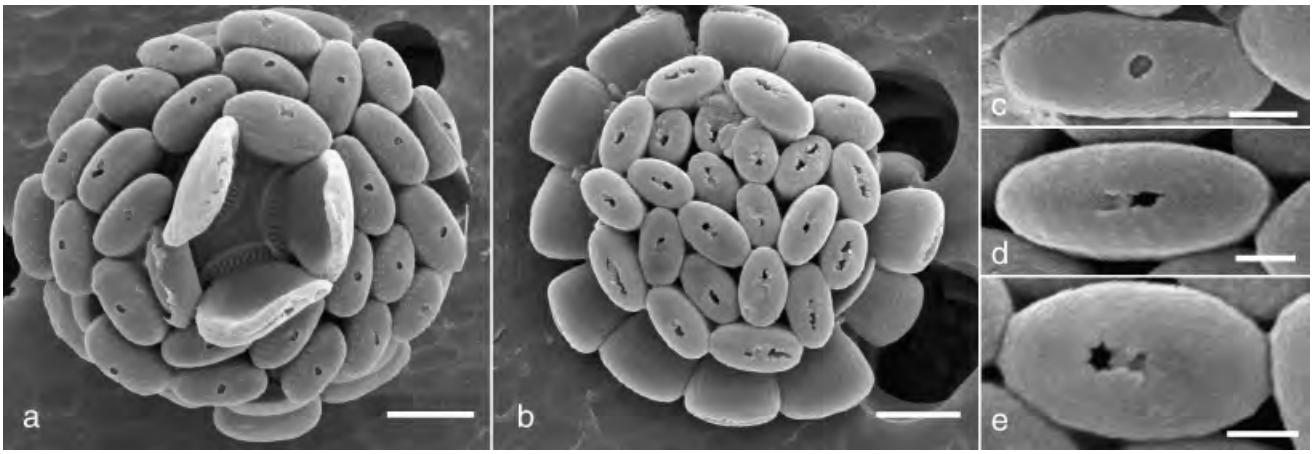

FIG. 2. Scanning electron micrographs of *Algirosphaera robusta* coccosphere and coccolith shape. (a) Coccosphere in apical view with three higher petalloid coccoliths surrounding the flagellar opening. Scale bar, 2 μm. (b) Coccosphere in antapical view with equatorial coccoliths collapsing to give a coronate profile. Scale bar, 2 μm. (c) Distal view of coccolith with parallel-sided profile. Scale bar, 0.5 μm. (d) Distal view of coccolith with flattened elliptical profile. Scale bar, 0.5 μm. (e) Distal view of coccolith with elliptical profile. Scale bar, 0.5 μm.

parallel sided to ellipsoidal (Fig. 2, c–e). Body coccoliths varied in height from 1.4 to 2.3 μm (average 1.9 μm, $n = 83$).

Coccolith structure was investigated by a combination of detailed high-resolution SEM of coccoliths including broken specimens, TEM of fixed samples, and LM. These observations indicate an unusually complex structure that can be divided into three parts: the baseplate scale, the base, and the hood.

The coccolith base consists of five cycles of elements with strong radial symmetry (Fig. 3, a–d). The rim is formed of an upper cycle of elements with radial sutures and a lower cycle with strong sinistral obliquity (Fig. 3, c and d). From the inner edge of the rim, a radial cycle of spokelike elements runs toward the center of the coccolith (Fig. 3, a, c, and d). The rim and radial cycles each have the same number of elements, and the radial cycle elements interdigitate with the lower rim elements around the inner margin of the rim (Fig. 3, c and d). The lamellar cycle consists of vertically directed elements, which morphologically form the base of the hood (Fig. 3, a and i). However, they alternate with the radial elements and are discrete from the main hood elements. Finally, a set of irregular proximal cover laths extends over the proximal surface of the coccoliths, inside the lamellar cycle (Fig. 3b). These primarily grow inward from the margin of the hood, but additional elements, not connected to the margin, occur in the center of the cycle. Examination of SEM micrographs of specimens in various orientations and preservation states suggests that each of these five cycles is a discrete set of crystal units (i.e., the different elements do not interconnect to form larger composite crystal units). In decalcified TEM sections, all these basal elements are completely lost, appearing as white holes (Fig. 3, i and j). Conversely, in sections in which the calcite has been preserved, they usually appear black (i.e., electron opaque) (Fig. 5a). This is typical of heterococcolith elements, indicating pure calcite without a substantial intracrystalline organic phase. The rhabdolith base is too small and thin to allow accurate LM observations of crystallographic orientation.

The hood consists of three sets of elements, each consisting of numerous small, discrete crystal units, not organized in discrete radial cycles: (1) On the outside there is a thin cycle of numerous cover tiles (Fig. 3, a, h, and i). These are imbricated, with lower tiles overlapping higher ones and tiles to the right overlapping those to the left, giving rise to an anticlockwise spiral arrangement. It has previously been assumed that this cycle extended inward to form the bulk of the hood; however, both SEM and TEM observations show that they only form a narrow (~0.02 μm) outer coating. (2) Beneath this cover, the bulk of the hood is formed of a mass of oblique rods (Fig. 3, e–k). These rods, typically 0.5–1 μm long and 0.05 μm in diameter, are oriented obliquely to the coccolith long axis and slope upwards in a counterclockwise sense at an angle of about 45°. They do not interconnect, and there is usually space between adjacent rods. The TEM sections cut the hood at varying angles and give the impression of variable orientations of these oblique elements (Fig. 3, i–k); however, SEM observation of broken specimens suggests that their orientation is rather constant (Fig. 3, f–h). Discrete sets of these elements occur on each side of the hood (Fig. 3, g and h). The SEM observations suggest that the lower/clockwise-directed end of the rods is abruptly truncated and that they taper distally (Fig. 3f), suggesting crystal growth in an upward direction. (3) Inside these oblique elements on either side of the hood, and thus delimiting the long sides of the central cavity, are discrete sets of vertical rods (Fig. 3, f, h, and k) of similar size to the oblique rods. These are arranged in several irregular overlapping tiers, rather than a single cycle extending

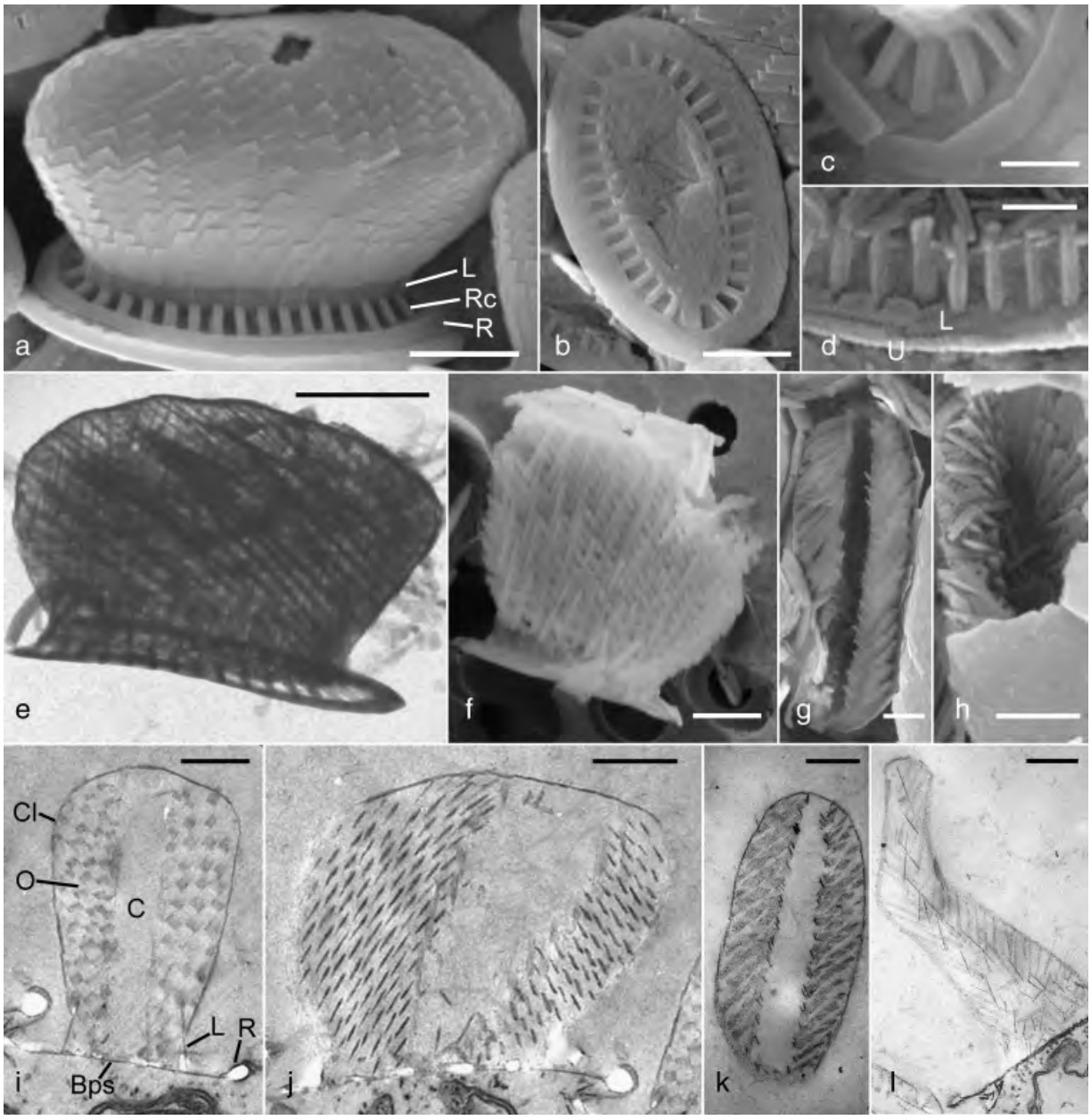

FIG. 3. *Algirosphaera robusta* coccolith structure. SEM: (a–d, f–h); TEM (e, i–l). (a) Side view of body rhabdolith showing rim (R), radial cycle (Rc), lamellar cycle (L), and coccolith hood. Scale bar, 0.5 μm. (b) Proximal view of coccolith showing irregular proximal cover laths. Scale bar, 0.5 μm. (c) Detail of coccolith rim. Scale bar, 0.2 μm. (d) Detail of broken specimen showing upper (U) and lower (L) rim cycles and radial cycle of spokelike elements. Scale bar, 0.2 μm. (e) Body rhabdolith showing complex internal structure of hood. Scale bar, 0.5 μm. (f) Broken specimen in side view showing oblique and vertical rods. Scale bar, 0.5 μm. (g) Broken specimen in distal view showing thick blades of oblique rods either side of central cavity. Scale bar, 0.5 μm. (h) Broken specimen in distal view showing vertical rods bordering the central cavity. Scale bar, 0.5 μm. (i) Coccolith sectioned perpendicularly to the axis of the central cavity showing base-plate scale (Bps), rim (R), lamellar cycle element (L), cover laths (Cl), oblique rods (O), and central cavity (C). Scale bar, 0.5 μm. (j) Coccolith sectioned at oblique angle to the axis of the central cavity. Scale bar, 0.5 μm. (k) Horizontal section of coccolith. Scale bar, 0.5 μm. (l) Section of stomatal coccolith. Scale bar, 0.5 μm.

from the proximal surface. They clearly taper upward (Fig. 3f), suggesting that growth extends in this direction. In decalcified TEM sections, the hood elements are still plainly visible, appearing gray, suggesting that they contain significant amounts of intracrystalline organic material (Fig. 3, i–l). This inference is supported by observations on preparations in which the calcite is preserved (Fig. 5a), in which the hood elements show lower opacity than the base elements. The oblique and vertical rods form two thick blades on either (long) side of the coccolith, separated by a cavity, leaving only the cover tiles extending around the distal

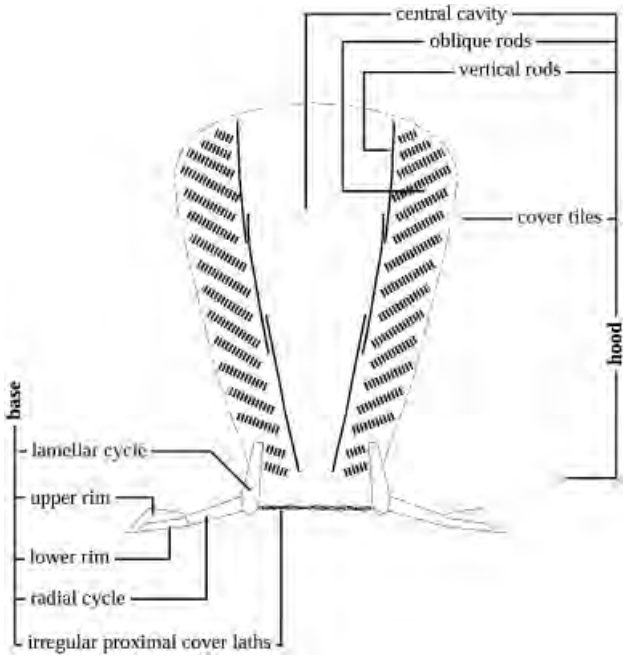

FIG. 4. Schematic representation of *Algirosphaera robusta* coccolith structure.

and lateral parts of the hood (Fig. 3, h and k). In the light microscope, the hood is very prominent, and observations with cross-polarized light and a gypsum plate clearly indicate that it is formed of crystals with the *c*-axis directed vertically (i.e., perpendicular to the base, not illustrated). This optical behavior is predominantly a product of the oblique rods, and it is not possible with such small coccoliths to determine if the cover plates and vertical rods have the same crystallographic orientation. The stomatal coccoliths are similar in ultrastructure to the body coccoliths but have extended hoods, which can be more than twice the height of the body coccoliths (Fig. 3l). A schematic representation of the structure of *A. robusta* coccoliths is presented in Fig. 4.

Cell ultrastructure: The internal organization of the cell shows many of the features characteristic of the Haptophyta (Fig. 5). Adjacent to the nucleus is a single Golgi body, the cisternae in the middle portion of the stack showing intercalary dilations characteristic of the haptophytes (Fig. 5b). The entire cytoplasm except the flagellar region is enclosed by the peripheral endoplasmic reticulum (PER), situated immediately beneath the plasmalemma. The single antapically positioned parietal chloroplast possesses lamellae of three thylakoids and contains an immersed fusiform pyrenoid, which is surrounded by a very thin membranous envelope (Fig. 5, c and d). The pyrenoid is traversed by several lamellae of two or three thylakoids. Girdle lamellae are not present in the chloroplast, the outer ER membrane of which is continuous with the nuclear membrane. Elongated sections of mitochondria with tubular cristae are often situated adjacent to the inner surface of the chloroplast. Body scales are produced in Golgi vesicles, two or more scales often observed within one vesicle toward the mature face of the stack (Fig. 6a).

The first stage in the process of coccolith formation in *A. robusta* is the production of the coccolith base-plate scale within a Golgi vesicle located on the distal face of the Golgi stack. This vesicle subsequently migrates toward the flagellar pole of the cell, reorienting as it approaches the PER such that the scale is eventually situated perpendicular to the plasma membrane and hence often to the long axis of the Golgi stack itself (Fig. 6a). From this early stage and throughout coccolithogenesis, coated vesicles of Golgi origin are frequently observed fusing with the coccolith-forming vesicle. Nucleation and growth of the calcite crystals that form the rim of the developing coccolith appear to commence as or soon after the vesicle starts to dilate to take the form of the future coccolith (Fig. 6b). The vesicle forms a T-shape in cross-section as the central area dilates away from the base-plate scale, at which stage it is filled with a substance that appears as a fine gray deposit (Fig. 6c). The shape of the expanding vesicle appears to be modeled by invaginations of the PER (Fig. 6, d and e) and sometimes also by proximity to storage vacuoles or vesicles containing fully formed coccoliths, both of which are themselves in close contact with the PER. The distal end of the coccolith vesicle branches out to form an interconnected matrix of tubes (Fig. 6d), which is intimately associated with the PER and also in close proximity to extensions of Golgi cisternae. This distal tubular matrix contains a dark granular substance that appears to be exported into the main compartment of the coccolith-forming vesicle (Fig. 6d). As the coccolith vesicle subsequently expands outward, the first sign of calcification of the rhabdolith hood involves thin threadlike crystallites (the cover laths) forming at the periphery of a central compartment, which is delimited by extensions of the intricate membrane system (Fig. 6e). The main phase of calcification of the rod elements of the hood then occurs. As noted above, there appears to be a significant organic component to the hood elements, and it appears that calcification occurs inside this matrix (Fig. 6, d–g). Growth of the crystals forming the oblique rods does not seem to be directional from the base upward as inferred from SEM observations. Membranes within the coccolith vesicle model the external shape of the forming coccolith (Fig. 6, e–h). During calcification, the coccolith vesicle typically closely surrounds the forming coccolith, but once fully formed, the close fit is lost (Fig. 6i) before extrusion of the coccolith to the coccosphere, which occurs in the apical region of the cell near the flagellar pole.

The structure of the flagellar apparatus and the haptonema of *A. robusta* shows marked similarities to that of *S. pulchra* Lohmann described by Inouye and Pienaar (1988). The terminology adopted in the following description is that of Beech and Wetherbee

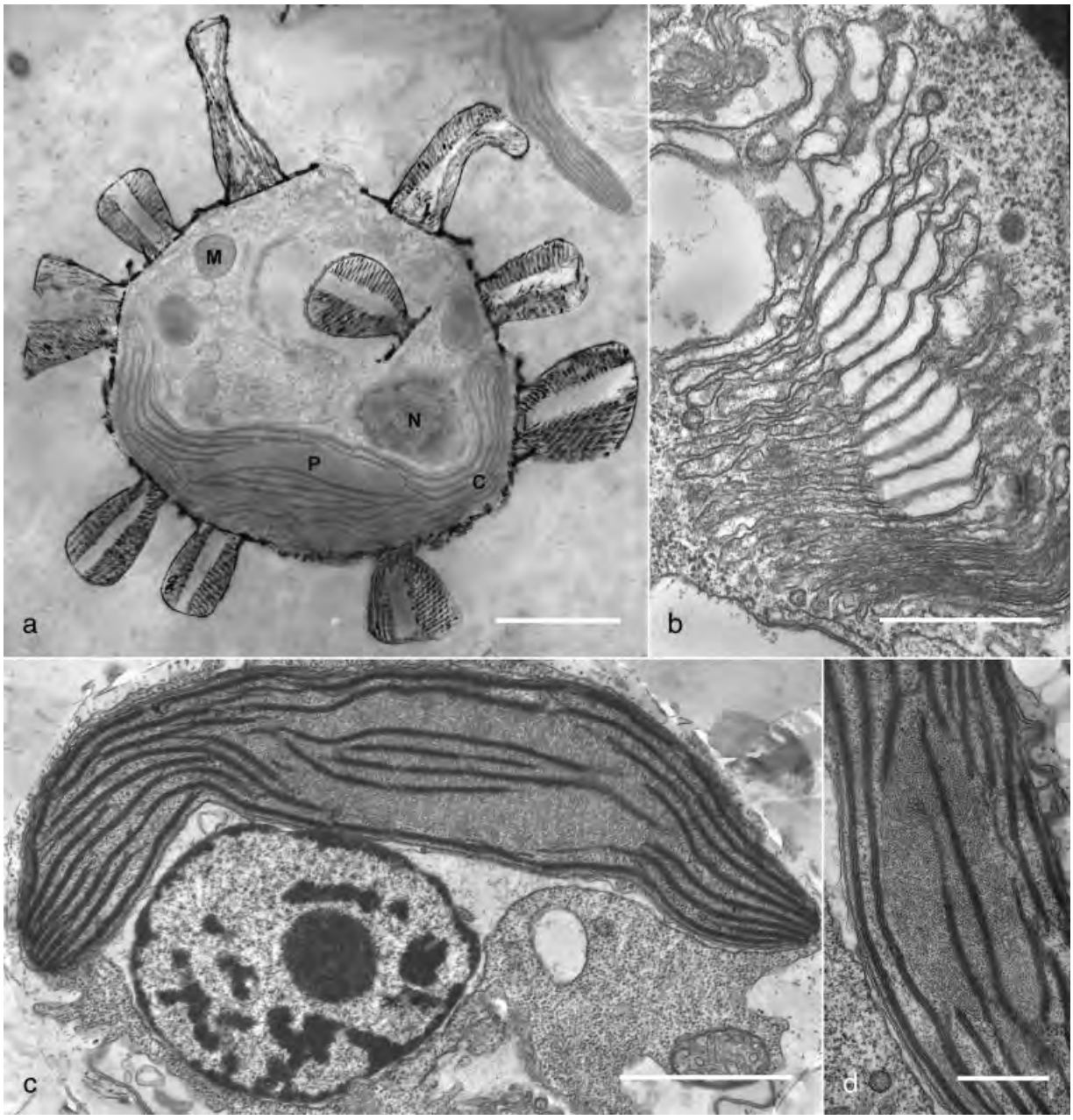

FIG. 5. *Algirosphaera robusta* general ultrastructure (TEM thin sections). (a) Median longitudinal section of whole cell with calcite preserved showing major cell components: nucleus (N), chloroplast (C), pyrenoid (P), and mitochondrion (M). Scale bar, 2 μm. (b) Golgi stack with dilations typical of haptophytes. Scale bar, 1 μm. (c) Nucleus and chloroplast enclosed within common membrane. Scale bar, 0.5 μm. (d) Detail of immersed pyrenoid. Scale bar, 0.2 μm.

(1988). The flagellar basal bodies, the lumen of which contain electron-dense cores as in *S. pulchra*, are joined by distal and proximal connecting bands, the former surrounded by an amorphous electron opaque material (Fig. 7, a–d). The haptonematal base consists of eight microtubules (Fig. 7, a and d), but only six of these microtubules (one less than in *S. pulchra*) extend into the emergent part of the haptonema where they are surrounded by PER to form a concentric structure when viewed in transverse section (Fig. 7e). The flagellar roots are of five types—four microtubular and one fibrous root. Root 1 (R1) is a sheetlike structure of about 10 microtubules, which arises close to the haptonematal base and extends for some distance away from the basal bodies immediately beneath the PER (Fig. 7, a–c, g, and h). Root 2 (R2), which arises between the two basal bodies, consists of four microtubules (Fig. 7, c and g–i). A fibrous root is also seen in close proximity to the right basal body (Fig. 7h). Like *S. pulchra*, *A. robusta* lacks the secondary

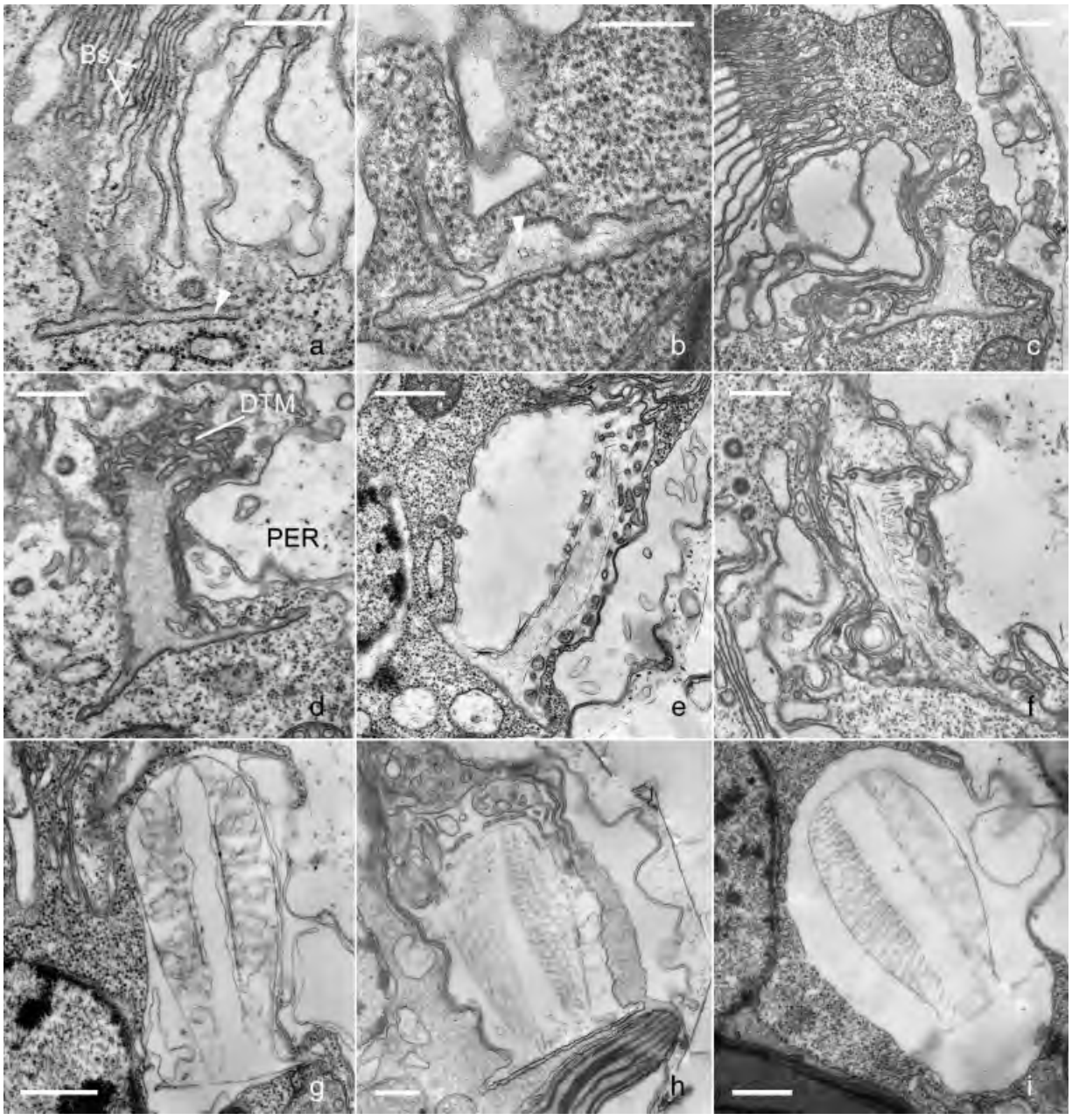

FIG. 6. Sequential TEM thin sections of *Algirosphaera robusta* coccolithogenesis. (a) Uncalcified base-plate scale in vesicle of Golgi origin (arrowhead). Note body scales (Bs) in vesicles in Golgi stack. (b) Early stage of calcification: rim crystal nucleation (arrowhead). (c) Central area of the vesicle dilates away from the base-plate scale. (d) The coccolith vesicle forms a distal tubular matrix (DTM) and remains in close proximity with the peripheral endoplasmic reticulum (PER). The cavity of the vesicle is filled with a fine granular substance. (e) As the coccolith vesicle dilates, calcification of the fine hood elements is initiated within a space delimited by membranes. (f) Main phase of hood calcification. (g) Membranes model the internal cavity and external shape of the coccolith. (h) Final stages of formation of the hood. (i) A fully formed coccolith just before extrusion from the cell. Scale bars, 0.5 μm.

microtubular bundles (crystalline roots) that are commonly associated with roots 1 and 2 in other coccolithophores. Roots 3 and 4, both initially consisting of two microtubules, arise on either side of the right basal body (Fig. 7j). Further from the right basal body, the number of microtubules in these two roots increases, and they join to form a root with seven microtubules (Fig. 7k).

DISCUSSION

Taxonomy and life cycle: Three species of *Algirosphaera* are identified by some authors based on coccosphere and coccolith shape. As morphologies corresponding to all three of these species occurred in our clonal culture, we fully support the conclusion of Kleijne (1992) that *A. oryza* and *A. bicornu* are

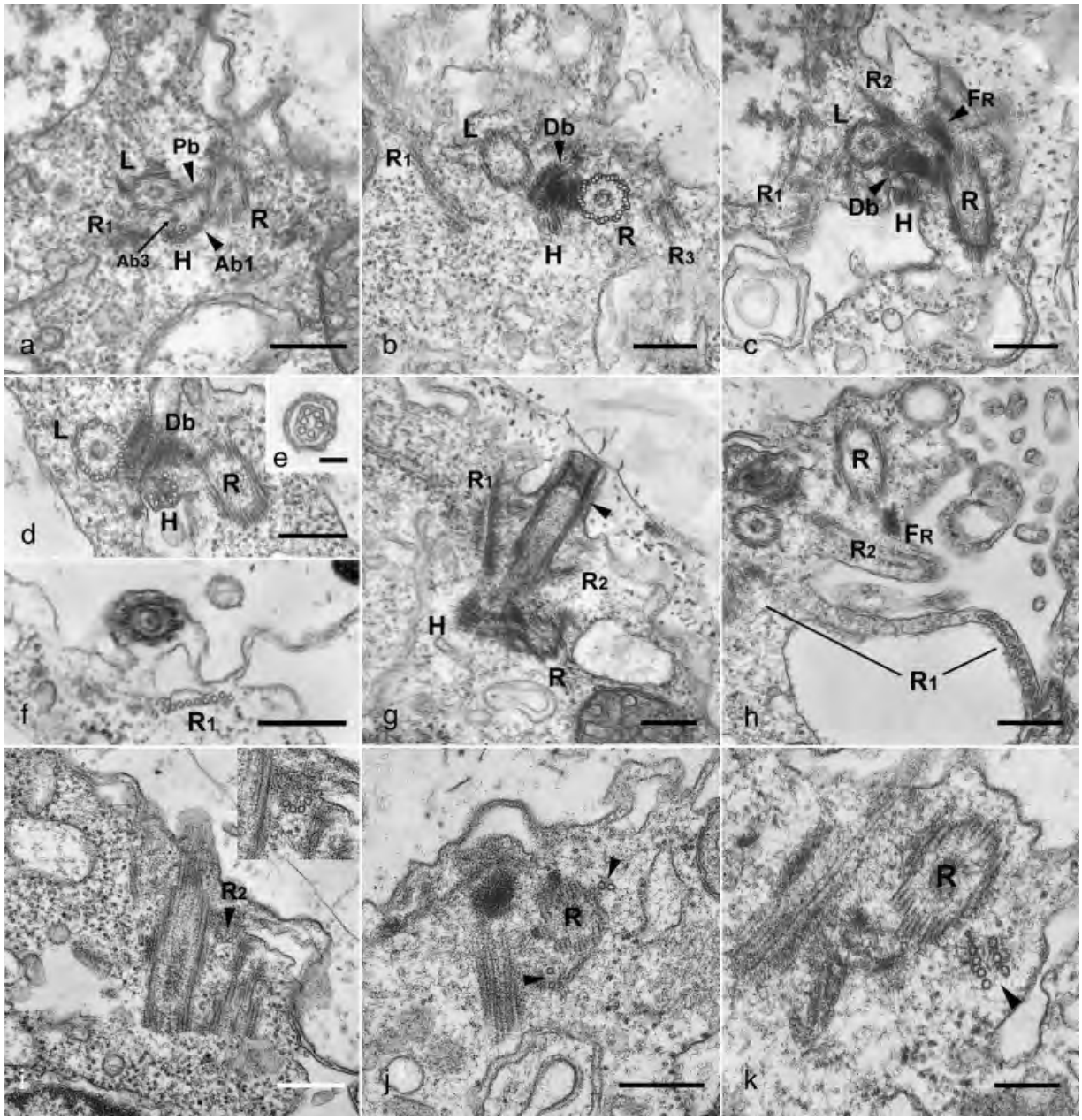

FIG. 7. *Algirosphaera robusta* flagellar base structure (TEM thin sections). (a–d) Representative transverse sections cut through the flagellar base region (all viewed from outside). Two basal bodies (L and R); proximal (Pb) and distal (Db) connecting bands; accessory connecting bands (Ab1, Ab3); the haptonematal base (H); microtubular roots 1 (R1), 2 (R2), 3 (R3); and a fibrous root (FR) are seen. Scale bars, 0.2 μm. (e) Transverse section of the haptonema containing ringlike endoplasmic reticulum and six microtubules. Scale bar, 0.1 μm. (f) Transverse section of the sheetlike microtubules of root 1 (R1). Scale bar, 0.2 μm. (g) Longitudinal section of the left flagellar base, root 1 (R1) and root 2 (R2). Note the axoneme (arrowhead). Scale bar, 0.2 μm. (h) Root 1 (R1) extending away from the flagellar bases. (i and inset) Transverse section of root 2 (R2), consisting of four microtubules. Scale bar, 0.2 μm. (j) Section of roots 3 and 4, each consisting of two microtubules (arrowheads) originating either side of the right basal body (R). Scale bar, 0.2 μm. (k) Section showing roots 3 and 4 joining to form a root consisting of seven microtubules (arrowhead) further from the right basal body (R). Scale bar, 0.1 μm.

junior synonyms of *A. robusta*. It should be noted that the wide temperature tolerance of this species in culture may account for its very broad biogeographic distribution, with reported occurrences from the sub-Arctic to the equator. Alternatively, two or more morphologically similar but ecologically and genetically distinct species may exist within *A. robusta*. This is a distinct possibility, given the recent documentation of widespread pseudocryptic speciation within the coccolithophores (Geisen et al. 2002, Sáez et al. 2003). We believe that the genus *Algirosphaera* should include at least two other, rare, species. *Algirosphaera*

meteora was described from isolated coccoliths in sediment samples, but it also occurs very rarely in plankton samples. The coccosphere of this species differs from *A. robusta* in being monomorphic and more broadly elliptical in plan view, with coccoliths having a different profile with a distinct constriction in the lower part, tapering distally, and exhibiting an open central area in proximal view (i.e., the irregular proximal cover laths are absent). *Algirosphaera cucullata* is usually included in *Cyrtosphaera* Kleijne, following Kleijne (1992), on the basis that the coccosphere is varimorphic. However, the structure of the coccoliths of this species has always been anomalous and is distinctly different from the type species of *Cyrtosphaera*, *C. aculeata* (Kamptner) Kleijne, because the central protrusion is formed of a mass of fine crystals, except for a proximal cycle of vertical lamellar elements. Our new observations on *A. robusta* indicate that these needle-like crystals are equivalent to the oblique rods in *A. robusta*, hence it was recombined into *Algirosphaera* by Young et al. (2003).

Recently, it has become clear that the typical haptophyte life cycle is haplo-diploid, with asexual mitotic reproduction occurring in both phases (Billard and Inouye 2004). Typically, for coccolithophores the diploid phase produces heterococcoliths and the haploid phase holococcoliths. Evidence for this comes from a limited set of culture observations (Houdan et al. 2004, Noel et al. 2004) supplemented by occasional observation in plankton samples of combination coccospheres, which are formed during the transition between the two phases (i.e., during or shortly after meiosis or syngamy) and so possess both holococcoliths and heterococcoliths. Among the Rhabdosphaeraceae, such combination coccospheres have been recorded for *Acanthoica quatrospina* by Cros et al. (2000) and for *R. clavigera* by Cros and Fortuño (2002). Combination coccospheres of *A. robusta* heterococcoliths with *Sphaerocalyptra quadridentata* holococcoliths were recorded by Kamptner (1941) from LM, and this life cycle association was recently confirmed by Triantaphyllou and Dimiza (2003) from SEM observations of further combination coccospheres.

Coccolith structure and formation: The structure of *A. robusta* coccoliths is in many ways much more complex than that of any other coccoliths described in detail to date and shows some very interesting differences from other coccoliths. The discussion below proceeds from the outer rim to the distal process, or hood, because this is the broad direction of coccolith growth and also the direction of increasing deviation from normal coccolith structure.

The outer rim structure shows typical heterococcolith features. It consists of a limited number of elements arranged in two cycles, with the same number of elements in each cycle, and it is formed by a growth process commencing with crystal nucleation around a protococcolith ring located on the margin of the base-plate scale. The TEM observations indicate that growth of the rim cycles occurs within an expanding coccolith vesicle and without a precursor matrix, and there is no evidence of intracrystalline organics. All of these features are typical of heterococcolith formation, as deduced from studies on species such as *Pleurochrysis carterae* (Braarud et Fagerland) Christensen and *Emiliania huxleyi* (Young et al. 1999). The outer rim structure is also similar to typical heterococccoliths in that it is formed of two cycles of intergrown, complex-shaped crystal units. In heterococcoliths of numerous other species, it has been demonstrated that the two rim cycles have very different crystallographic orientations, typically subvertical and subradial (V/R model of Young et al. 1992). In *A. robusta*, we have not been able to determine the orientation of crystals in the coccolith base due to their small size, but we predict that the outer rim structure will not prove atypical.

The other basal cycles (radial cycle, lamellar cycle, irregular proximal cover laths) appear to be separately nucleated crystal units and show a distinctive departure from the standard V/R model of coccolith biomineralization. Three features, however, indicate that these elements are formed by a modified mode of typical heterococcolith biomineralization rather than a total departure from this model: (1) the common origin of the radial cycle with the rim cycles, (2) the one-to-one correspondence of elements in the radial and lamellar cycles, and (3) the absence of intracrystalline organics in all these cycles. In *A. robusta*, the radial laths are separate from the rim elements, but inserted between, as has been described in *S. pulchra* by Young et al. (2004).

The sacculiform process of the coccolith shows much stronger departures from normal heterococcolith biomineralization: in particular, (1) structurally, the hood is formed of numerous discrete, simple crystal units, each evidently separately nucleated, rather than cycles of complex crystal units originating from a protococcolith ring; (2) TEM observations suggest that a significant intracrystalline organic phase occurs within the hood elements; and (3) TEM observations of progressive coccolith growth stages indicate that biomineralization of the hood does not occur by growth from the base upward, but rather by simultaneous calcification throughout the hood within a precursor organic matrix. Taken together, these features indicate that biomineralization of the hood shows very few of the typical features of heterococcolith biomineralization, and thus it is reasonable to infer that it is formed by a discrete biomineralization mode with significantly different biochemical regulatory processes and controlling sets of genes.

The hood structure of *Algirosphaera* has previously been assumed to be directly homologous to the processes of other Rhabdosphaeraceae (Kleijne 1992, Aubry 1999). However, the spines of *Rhabdosphaera* Haeckel and *Acanthoica* Lohmann emend. Schiller emend. Kleijne and the trumpet-shaped processes of *Discosphaera* Haeckel are formed of a single set of small spirally arranged crystals, without the

complex internal structure of the *Algirosphaera* hood. A direct homology seems unlikely (i.e., it does not appear reasonable to argue that any one of the three types of elements present in the *Algirosphaera* hood represents a modification of the cycles present in, e.g., the *Discosphaera* trumpet). However, if the inference that the hood is formed by a novel biomineralization mode is accepted, then a possible explanation for the diversity of these structures, and those of the fossil Rhabdosphaeraceae, becomes available. Arguably, this mode is more flexible than the normal heterococcolith biomineralization mode, with different sets of cycles being produced according to morphological need. On this basis, we can predict that all the diverse process structures of the Rhabdosphaeraceae are produced by the same type of biomineralization mode, characterized by shape determination from an organic precursor, dispersed nucleation, and involvement of an organic matrix. Among extant and Cenozoic coccolithophores, spines and processes formed of numerous small elements suggesting dispersed nucleation occur only in the Syracosphaeraceae and Rhabdosphaeraceae. Hence, this new biomineralization mode may be confined to these two families, supporting other evidence for the apparent affinity of the two families. Among Mesozoic coccolithophores, this type of structure is observed in many other, extinct, families (e.g., Podorhabdaceae, Zeugrhabdotaceae), where it may prove a useful phylogenetic character.

In all heterococcolithophores studied to date, the coccoliths are produced inside the cell within Golgi-derived vesicles. However, as an increasing number of species are examined in detail, diversity is becoming apparent in this process, notably in the manner in which components for the construction of the coccolith are transported to the vesicle and in the role of different cell components in shaping the forming coccolith. Morphological and biochemical aspects of coccolith production have been extensively studied in two model coccolithophore species, *E. huxleyi* and *P. carterae*. The organic base-plate within the coccolith production compartment in *E. huxleyi* is positioned closely apposed to the nuclear membrane and exhibits the same curvature as the nucleus (Klaveness 1972). A reticular body of anastomizing tubes directly linked to the coccolith vesicle may be involved in the transfer of precursor organic and mineral components from the Golgi body and possibly other vesicles to the coccolith vesicle (Westbroek et al. 1984). In *P. carterae*, the vesicle containing the coccolith base-plate scale is transferred to a more distal region between the nucleus and the plasma membrane, and numerous Golgi-derived vesicles containing densely staining granules termed "coccolithosomes" (Outka and Williams 1971) transport both calcium ions (van der Wal et al. 1985) and polysaccharides (van der Wal et al. 1983) to the coccolith vesicle. In *Umbilicosphaera sibogae* var. *foliosa*, the ER system together with the nucleus and Golgi body seem to play roles in determining the shape of the coccolith vesicle (Inouye and Pienaar 1984). The process of coccolith production in *A. robusta* is unusual in that the coccolith vesicle is located at the periphery of the cell, and the PER appears to play an important role. The reticular body of *E. huxleyi* and the distal tubular matrix of *A. robusta* have certain morphological characteristics in common (both are tubular structures of ER origin), and some degree of analogy in their function seems likely. The exact function of the PER in haptophytes has not been elucidated, but as the extensive membrane system of the reticular body in *E. huxleyi* is believed to transport calcium ions (and other precursor elements) into the lumen of the coccolith vesicle, and as these ions presumably pass through the PER during the uptake process, direct involvement of a PER-derived structure in coccolith formation, as observed in *A. robusta*, may have functional and energetic advantages. Coccolith formation was not focused on in the cytological study of *S. pulchra* by Inouye and Pienaar (1988), but examination of their figures 17 and 18 indicate that, as in *A. robusta*, the coccolith vesicle is located in close contact with the PER.

Cell ultrastructure: Kawachi and Inouye (1994) defined two types of flagellar root system in the coccolithophores based on the presence or absence of the secondary crystalline roots associated with R1 and R2: the *Pleurochrysis* type characterized by two well-developed crystalline roots, and the *Syracosphaera* type for species lacking CR1 and CR2. Sym and Kawachi (2000) defined a third intermediary group for species possessing only one crystalline root. The flagellar root system of *A. robusta* is clearly very similar to that of *S. pulchra*, including the absence of crystalline roots CR1 and CR2. The *Syracosphaera* type, now including these two species, is more characteristic of noncoccolithophore haptophytes and hence may indicate an early divergence during coccolithophore evolution for the Rhabdosphaeraceae/Syracosphaeraceae.

While the similarity in many ultrastructural features of *A. robusta* and *S. pulchra* is indicative of a close evolutionary relationship between the Rhabdosphaeraceae and the Syracosphaeraceae, ultrastructural differences are observed, notably in the size and ornamentation of the noncalcified organic body scales. The body scales of *S. pulchra* exhibit the typical pattern (radiating and concentric microfibrils) and are of a typical size (~2 μm) for coccolithophores (Inouye and Pienaar 1988). *Algirosphaera robusta* body scales, in contrast, apparently have only a radiating pattern of microfibrils, possess an accentuated rim and central structure, and are an order of magnitude smaller (~0.2 μm), a size more closely matching that of the haptonematal scales present in certain haptophyte species. There is a lack of cytological information for other members of the Rhabdosphaeraceae and the Syracosphaeraceae, but it seems that body-scale morphology is a relatively highly variable (i.e., rapidly evolving) character and hence may prove to be useful for resolving fine-scale phylogeny.

CONCLUSION

Successful isolation of *A. robusta* from a sample from the deep chl maximum suggests that deep photic species may present fewer problems for culture work than has been suggested. Given the growing recognition of the importance of deep photic species in oceanic ecology, we suggest that a targeted isolation program for such species would be justified. Culture observations support the previous inference of Kleijne (1992) that the commonly recognized species *A. oryza*, *A. robusta*, and *A. quadricornu* are conspecific, all three morphotypes occurring in our clonal culture. However, *A. meteora* and *A. cucullata* are recognized as discrete species. In terms of flagellar root structure, *A. robusta* shows stronger affinities with *S. pulchra* than with any other cytologically described coccolithophore, supporting previous tentative suggestions of affinity between the Rhabdosphaeraceae and Syracosphaeraceae based on coccolith structure (presence of a radial lath cycle and disjunct central processes). Both coccolith morphology and cytological observations of coccolith formation suggest that the hood of *Algirosphaera* coccoliths is formed by a distinctive biomineralization mode in which calcification occurs through dispersed nucleation within a precursor organic matrix. The paradigmatic V/R model of heterococcolith biomineralization (Young et al. 1992, 1999) has been extremely successful as a tool for interpreting homology in coccolith structure, but in this case, it is only applicable to the rim structure. Our new observations show that the "problematic" central area structures of *Algirosphaera* are not formed by a modified version of the V/R biomineralization process, but by a significantly different process, probably with different biochemical pathways and certainly with less evolutionarily conserved features, and so with less ability to infer homology. Young et al. (1999) previously showed that heterococcolith V/R biomineralization and holococcolith biomineralization constitute discrete biomineralization modes. Our new observations complicate this pattern by adding a third biomineralization mode, present only in a limited subset of coccolithophores. *Algirosphaera robusta* is thus a particularly interesting candidate for biochemical and genomic studies of biomineralization processes in comparison with *E. huxleyi*.

This research was funded by the EU TMR network ERBFMRX CT97 0113 CODENET (Coccolithophorid Evolutionary Biodiversity and Ecology Network) and by the French Agence National de la Recherche/Institut Français de la Biodiversité ANR-05-BDIV-004 BOOM (Biodiversity of Open Ocean Microcalcifiers) project. Numerous colleagues assisted in the study and shared insights, notably Annelies Kleijne (VU, Amsterdam) and Lluisa Cros (CSIC, Barcelona). Didier Goux and Jacques Prigent (EM unit, University of Caen) as well as Alex Ball and Chris Jones (EMMA unit, NHM) provided invaluable assistance with the electron microscope studies.

Aubry, M.-P. 1999. *Handbook of Cenozoic Calcareous Nannoplankton. Book 5: Heliolithae (Zygoliths and Rhabdoliths)*. Micropalaeontology Press, American Museum of Natural History, New York, 368 pp.

Beech, P. L. & Wetherbee, R. 1988. Observations on the flagellar apparatus and peripheral endoplasmic reticulum of the coccolithophorid, *Pleurochrysis carterae* (Prymnesiophyceae). *Phycologia* 27:142–58.

Billard, C. & Inouye, I. 2004. What's new in coccolithophore biology? *In* Thierstein, H. R. & Young, J. R. [Eds.] *Coccolithophores: From Molecular Processes to Global Impact*. Springer Verlag, Berlin, pp. 1–30.

Cros, L. & Fortuño, J.-M. 2002. Atlas of NW Mediterranean coccospheres. *Sci. Mar.* 66(Suppl. 1), 186 pp.

Cros, L., Kleijne, A., Zeltner, A., Billard, C. & Young, J. R. 2000. New examples of holococcolith–heterococcolith combination coccospheres and their implication for coccolithophorid biology. *Mar. Micropaleontol.* 39:1–34.

Gaarder, K. R. & Hasle, G. R. 1971. Coccolithophorids of the Gulf of Mexico. *Bull. Mar. Sci.* 21:519–44.

Geisen, M., Billard, C., Broerse, A. T. C., Cros, L., Probert, I. & Young, J. R. 2002. Life-cycle associations involving pairs of holococcolithophorid species: intraspecific variation or cryptic speciation? *Eur. J. Phycol.* 37:531–50.

Hagino, K., Okada, H. & Matsuoka, H. 2000. Spatial dynamics of coccolithophore assemblages in the equatorial Western-Central Pacific Ocean. *Mar. Micropaleontol.* 39:53–72.

Halldal, P. & Markali, J. 1955. Electron microscope studies on coccolithophorids from the Norwegian Sea, the Gulf Stream and the Mediterranean. *Avh. Norske Vidensk. Akad. I. Mat. Nat. Kl.* 1955:1–30.

Heimdal, B. R. 1993. Modern coccolithophorids. *In* Tomas, C. [Ed.] *Marine Phytoplankton: A Guide to Naked Flagellates and Coccolithophorids*. Academic Press, San Diego, CA, USA, pp. 147–247.

Houdan, A., Billard, C., Marie, D., Not, F., Sáez, A. G., Young, J. R. & Probert, I. 2004. Flow cytometric analysis of relative ploidy levels in holococcolithophore–heterococcolithophore (Haptophyta) life cycles. *Syst. Biodivers.* 1:14–28.

Inouye, I. & Pienaar, R. N. 1984. New observations on the coccolithophorid *Umbilicosphaera sibogae* var. *foliosa* (Prymnesiophyceae) with reference to cell covering, cell structure and flagellar apparatus. *Br. Phycol. J.* 19:357–69.

Inouye, I. & Pienaar, R. N. 1988. Light and electron microscope studies of the type species of *Syracosphaera*, *S. pulchra* (Prymnesiophyceae). *Br. Phycol. J.* 23:205–17.

Jordan, R. W. & Green, J. C. 1994. A check-list of the extant Haptophyta of the world. *J. Mar. Biol. Assoc. U. K.* 74:149–74.

Jordan, R. W. & Winter, A. 2000. Assemblages of coccolithophorids and other living microplankton off the coast of Puerto Rico during January–May 1995. *Mar. Micropaleontol.* 39:113–30.

Kamptner, E. 1941. Die Coccolitheenen der Sudwestküste von Istrien. *Ann. Naturh. Mes. Wien.* 51:54–149.

Kawachi, M. & Inouye, I. 1994. Observations on the flagellar apparatus of a coccolithophorid, *Cruciplacolithus neohelis* (Prymnesiophyceae). *J. Plant Res.* 107:53–62.

Keller, M. D., Selvin, R. C., Claus, W. & Guillard, R. R. L. 1987. Media for the culture of oceanic ultraphytoplankton. *J. Phycol.* 23:633–7.

Klaveness, D. 1972. *Coccolithus huxleyi* (Lohmann) Kamptner. I. Morphological investigations on the vegetative cell and the process of coccolith formation. *Protistologica* 8:335–46.

Kleijne, A. 1992. Extant Rhabdosphaeraceae (coccolithophorids, class Prymnesiophyceae) from the Indian Ocean, Red Sea, Mediterranean Sea and North Atlantic Ocean. *Scr. Geolog.* 100:1–63.

Loeblich, A. R. Jr. & Tappan, H. 1963. Type fixation and validation of certain calcareous nanoplankton genera. *Proc. Biol. Soc. Wash.* 76:191–6.

Marsh, M. E. 1999. Coccolith crystals of *Pleurochrysis carterae*: crystallographic faces, organisation, and development. *Protoplasma* 207:54–66.

Noel, M.-H., Kawachi, M. & Inouye, I. 2004. Induced dimorphic life cycle of a coccolithophorid, *Calyptrosphaera sphaeroidea* (Prymnesiophyceae, Haptophyta). *J. Phycol.* 40:112–29.

Norris, R. E. 1984. Indian Ocean nanoplankton. I. Rhabdosphaeraceae (Prymnesiophyceae) with a review of extant taxa. *J. Phycol.* 20:27–41.

Okada, H. & McIntyre, A. 1977. Modern coccolithophores of the Pacific and North Atlantic Oceans. *Micropaleontology* 23: 1–55.

Outka, D. E. & Williams, D. C. 1971. Sequential coccolith morphogenesis in *Hymenomonas carterae*. *J. Protozool.* 18:285–97.

Perch-Nielsen, K. 1985. Cenozoic calcareous nanofossils. *In* Bolli, H. M., Saunders, J. B. & Perch-Nielsen, K. [Eds.] *Plankton Stratigraphy.* Cambridge University Press, Cambridge, UK, pp. 427–554.

Sáez, A. G., Probert, I., Quinn, P., Young, J. R., Geisen, M. & Medlin, L. K. 2003. Pseudocryptic speciation in coccolithophores. *Proc. Natl. Acad. Sci. U. S. A.* 100:7163–8.

Sáez, A. G., Probert, I., Young, J. R. & Medlin, L. K. 2004. A review of the phylogeny of the Haptophyta. *In* Thierstein, H. R. & Young, J. R. [Eds.] *Coccolithophores: From Molecular Processes to Global Impact*. Springer Verlag, Berlin, pp. 251–70.

Shafik, S. 1989. Some new calcareous nannofossils from Upper Eocene and Lower Oligocene sediments in the Otway Basin, southeastern Australia. *Alcheringia* 13:69–83.

Steinmetz, J. C. 1991. Calcareous nannoplankton biocoenosis: sediment trap studies in the equatorial Atlantic, central Pacific and Panama Basin. *Ocean Biocoenosis Ser.* 1:1–85.

Stoll, H. M., Klaas, C., Probert, I., Ruiz-Encinar, J. & Garcia-Alonso, J. I. 2002. Calcification rate and temperature effects on Sr partitioning in coccoliths of multiple species of coccolithophorids in culture. *Global Planet Change* 34:153–71.

Sym, S. & Kawachi, M. 2000. Ultrastructure of *Calyptrosphaera radiata*, sp. nov. (Prymnesiophyceae, Haptophyta). *Eur. J. Phycol.* 35:283–93.

Tappan, H. 1980. *The Paleobiology of Plant Protists*. Freeman, San Francisco, 1028 pp.

Thiery, J.-P. 1967. Mise en évidence des polysaccharides sur coupes fines en microscopie électronique. *J. Microscopie* 13:119–36.

Triantaphyllou, M. V. & Dimiza, M. D. 2003. Verification of the *Algirosphaera robusta–Sphaerocalyptra quadridentata* (coccolithophores) life-cycle association. *J. Micropalaeontol.* 22:107–11.

van der Wal, P., de Bruijn, W. C. & Westbroek, P. 1985. Cytochemical and X-ray microanalysis studies of intracellular calcium pools in scale-bearing cells of the coccolithophorid *Emiliania huxleyi*. *Protoplasma* 124:1–9.

van der Wal, P., de Jong, E. W., Westbroek, P., de Bruijn, W. C. & Mulder-Stapel, A. A. 1983. Polysaccharide localization, coccolith formation, and Golgi dynamics in the coccolithophorid *Hymenomonas carterae*. *J. Ultrastruct. Res.* 85:139–58.

van Lenning, K., Probert, I., Latasa, M., Estrada, M. & Young, J. R. 2004. Pigment analyses and applications to chemotaxonomic studies of haptophytes. *In* Thierstein, H. R. & Young, J. R. [Eds.] *Coccolithophores: From Molecular Processes to Global Impact*. Springer Verlag, Berlin, pp. 51–74.

Varol, O. 1989. Eocene calcareous nannofossils from Sile (northwest Turkey). *Revta. Esp. Micropaleontol.* 21:273–320.

Westbroek, P., De Jong, E. W., Van Der Wal, P., Borman, A. H., de Vrind, J. P. M., de Bruijn, W. C. & Parker, S. B. 1984. Mechanisms of calcification in the marine alga *Emiliania huxleyi*. *Phil. Trans. R. Soc. London* 304B:435–44.

Young, J. R. 1993. The description and analysis of coccolith structure. *In* Hamrsmid, B. & Young, J. R. [Eds.] *Nannoplankton Research. Proceedings of the 4th INA Conference. Prague. Knihovnicka ZPN 14a*. MND Hodonín, Hodonín, Czech Republic, pp. 35–71.

Young, J. R. 1998. Neogene. *In* Bown, P. R. [Ed.] *Calcareous Nannofossil Biostratigraphy.* Chapman & Hall, London, pp. 225–65.

Young, J. R., Davis, S. A., Bown, P. R. & Mann, S. 1999. Coccolith ultrastructure and biomineralisation. *J. Struct. Biol.* 126:195–215.

Young, J. R., Didymus, J. M., Bown, P. R., Prins, B. & Mann, S. 1992. Crystal assembly and phylogenetic evolution in heterococcoliths. *Nature* 356:516–8.

Young, J. R., Geisen, M., Cros, L., Kleijne, A., Probert, I. & Ostergaard, J. B. 2003. A guide to extant coccolithophore taxonomy. *J. Nannoplankton Res.* 1(Special issue):1–132.

Young, J. R., Henriksen, K. & Probert, I. 2004. Structure and morphogenesis of the coccoliths of CODENET species. *In* Thierstein, H. R. & Young, J. R. [Eds.] *Coccolithophores: From Molecular Processes to Global Impact*. Springer Verlag, Berlin, pp. 191–216.

Ziveri, P., Stoll, H. M., Probert, I., Klaas, C., Geisen, M., Ganssen, G. M. & Young, J. R. 2003. Stable isotope "vital effects" in coccolith calcite. *Earth Planet. Sci. Lett.* 210:137–49.